Separation Science and Technology
Publication details, including instructions for authors and subscription information:
http://www.informaworld.com/smpp/title~content=t713708471

Modified Gel-Polarization Model for Ultrafiltration in Hollow-Fiber Membrane Modules

Ho-Ming Yeh[a]
[a] DEPARTMENT OF CHEMICAL ENGINEERING, TAMKANG UNIVERSITY, TAMSUI, TAIWAN, REPUBLIC OF CHINA

To cite this Article Yeh, Ho-Ming(1996) 'Modified Gel-Polarization Model for Ultrafiltration in Hollow-Fiber Membrane Modules', Separation Science and Technology, 31: 2, 201 — 211

To link to this Article: DOI: 10.1080/01496399608000690

URL: http://dx.doi.org/10.1080/01496399608000690

SEPARATION SCIENCE AND TECHNOLOGY, 31(2), pp. 201–211, 1996

Modified Gel-Polarization Model for Ultrafiltration in Hollow-Fiber Membrane Modules

HO-MING YEH
DEPARTMENT OF CHEMICAL ENGINEERING
TAMKANG UNIVERSITY
TAMSUI, TAIWAN, REPUBLIC OF CHINA

ABSTRACT

The effects of operating conditions on the permeate flux for the ultrafiltration of an aqueous solution of dextran T500 in hollow-fiber membrane modules have been investigated based on the modified gel-polarization model. It is found in this study that the present modified model successfully correlates the experimental results obtained under a lower transmembrane pressure while the conventional model only applies to operation under a high transmembrane pressure. It is believed that this model would be suitable for most membrane ultrafiltration systems.

INTRODUCTION

Ultrafiltration has become an increasingly important separation process for the concentration, purification, or dewatering of macromolecular and colloidal species in solution. Porter and Michaels (1–5) reviewed the applications in concentrations of milk, egg white, juice, pectin, and sugar, and in the recovery of protein from cheese whey, animal blood, gelatin, and glue. One of the common ultrafiltration designs is the hollow-fiber configuration in which the membrane is formed on the inside of tiny polymer cylinders that are then bundled and potted into a tube-and-shell arrangement. The rapid development of this process was made possible by the advent of an anisotropic, high-flux membrane capable of distinguishing among molecular and colloided species in the 10 Å to 10 μm size range.

Since this is a pressure-driven membrane separation process, the pressure applied to the working fluid provides the driving potential to force the solvent to flow through the membrane. Typical driving pressures for ultrafiltration systems are in the 10 to 100 psi range. For small applied pressures, the solvent flux through the membrane is proportional to the applied pressure. However, as the pressure is increased further, the flux begins to drop below that which would result from a linear flux–pressure behavior. Eventually, a limiting flux is reached where any further pressure increase no longer results in any increase in flux.

The reason for a limiting flux is that the high flux of retained solutes to the membrane surface leads to the well-known phenomena of concentration polarization. Under high-pressure operation, the concentration at the membrane surface can even rise to a point of incipient gel precipitation, forming a dynamic secondary membrane on top of the primary structure. The phenomenon of concentration polarization is common to all membrane processes. The first model proposed to explain the effect of polarization in ultrafiltration was the "gel polarization" model, first put forward by Michaels (6) and later developed by Porter (7). The basic assumption of this model is that beyond a certain value of applied pressure, the membrane permeation rate is limited by the presence of a gel layer deposited on the membrane, which increases the effective membrane thickness and reduces its hydraulic permeability. The second assumption, which is implicit in the traditional version of this model, is that the osmotic pressure of macromolecular solutions is always negligible. The secondary assumption is only valid for macromolecular solutions at very low concentrations; at high concentrations the osmotic pressure can be of the same order of magnitude as the applied pressure generally used in ultrafiltration (8, 9).

Since the gel polarization model only applies to membrane ultrafiltration under high-pressure operation where a limiting flux is reached, practical application is limited. It is the purpose of this work to modify this model so that its applications can be extended to the whole range of transmembrane pressure.

THEORY

Gel Polarization Model

In hollow-fiber membrane ultrafiltration processes, solutes that are rejected by the membrane accumulate on the membrane surface and form a concentration polarization layer there. At steady state the quantity of solutes conveyed by the solvent to the membrane is equal to those that diffuse back. Since the rejection of ultrafiltration for macromolecules is generally very high, the solute concentration in the permeate may be neglected. Accordingly, a material balance for the solute results in the socalled concentration polarization model

$$J_v = k \ln \frac{C_m}{C_b} \tag{1}$$

where J_v denotes the volume flux through the membrane, C_m and C_b are solute concentrations at membrane surface and in the bulk fluid, respectively, and k is the average mass-transfer coefficient.

The Graetz solutions (10) for convective heat transfer in laminar flow channels, suitably modified for mass transfer, may be used to evaluate the mass-transfer coefficient in a hollow fiber:

$$k = 1.62 \left(\frac{u_b D^2}{2r_m L}\right)^{1/3}, \qquad 100 < \mathrm{ReSe}\,\frac{2r_m}{L} < 5000 \tag{2}$$

where u_b is the bulk velocity of the fluid, D is the diffusion coefficient, r_m and L are the radius and length of a hollow fiber, respectively, and Re and Sc are the Reynolds and Schmidt numbers, respectively.

Under high-pressure operation the concentration at the membrane surface can even rise to point of incipient gel precipitation. When the membrane surface concentration is very high and a gel layer is formed, any further pressure increase no longer results in any increase in flux. In this case, gel layer concentration C_g is employed instead of C_m, and Eq. (1) becomes the gel polarization model

$$J_{v,\mathrm{lim}} = k \ln \frac{C_g}{C_b} \tag{3}$$

where $J_{v,\mathrm{lim}}$ denotes the limiting flux. It is shown by Eq. (3) that $J_{v,\mathrm{lim}}$ becomes zero as the solute concentration in the bulk fluid C_b approaches the gel concentration C_g.

In this conventional gel polarization model, the concentration of the gel layer may be considered to be constant and dependent only on the kinds of solute and membrane used. It is seen from Eq. (3) that the permeate flux $J_{v,\mathrm{lim}}$ obtained in the gel polarization model is independent of transmembrane pressure, and thus the gel polarization model is not quite suitable for analysis of membrane ultrafiltration.

Modified Gel-Polarization Model

Since membrane ultrafiltration is a pressure-driven separation process, the permeate flux J_v is observed to be proportional to the transmembrane pressure ΔP for small applied pressures. Therefore, when there is an absence of transmembrane pressure, no permeation occurs, while limiting permeate flux exists when the transmembrane pressure becomes sufficiently large. Accordingly, we may define the relation

$$J_v = \frac{\Delta P}{R + (\Delta P/J_{v,\text{lim}})} \tag{4}$$

which satisfies the following conditions:

$$\text{as } \Delta P \text{ is small,} \quad J_v = \frac{\Delta P}{R} = (\text{constant})\, \Delta P \tag{5}$$

$$\text{as } \Delta P = 0, \quad J_v = 0 \tag{6}$$

$$\text{as } \Delta P \rightarrow \infty, \quad J_v = J_{v,\text{lim}} \tag{7}$$

In Eq. (4), R is a constant.

Actually, Eq. (4) is another expression of the following resistance-in-series model for membrane ultrafiltration (11–13):

$$J_v = \frac{\Delta P}{R_m + R_f + R_p} \tag{8}$$

where R_m denotes the intrinsic resistance of a membrane, R_p and R_f are, respectively, the resistances due to the concentration polarizational gel layer and those due to other fouling phenomena such as solute adsorption, and ΔP in Eq. (4) and (8) is the transmembrane pressure defined as

$$\Delta P = \frac{P_L + P_0}{2} - P_p \tag{9}$$

where P_L and P_0 are, respectively, the outlet and inlet pressures of the tubeside and P_p is the permeate pressure of the shellside.

R_p will be proportional to the amount and the specific hydraulic resistance of the deposited layer. Since the deposited layer is compressible, R_p increases when ΔP increases or $J_{v,\text{lim}}$ decreases. Accordingly, we may write, from Eqs. (4) and (8):

$$R_p = \frac{\Delta P}{J_{v,\text{lim}}} \tag{10}$$

and accordingly,

$$R = R_m + R_f \tag{11}$$

Determination of R and $J_{v,\text{lim}}$

Equation (4) can be rewritten as

$$\frac{1}{J_v} = \frac{1}{J_{v,\text{lim}}} + \frac{R}{\Delta P} \tag{12}$$

Thus, this modified gel-polarization model will be true if a straight line of $1/J_v$ vs $1/\Delta P$ can be constructed from the experimental data at a certain feed flow velocity u_0 and feed concentration C_0 by the least-squares method. If that happens, the limiting permeate flux $J_{v,\text{lim}}$ as well as the combined membrane resistance R (including the intrinsic resistance of a membrane and the resistance due to solute adsorption) can be determined because $1/J_{v,\text{lim}}$ is the intersection at the ordinate and R is the slope of this straight line. In this case, both $J_{v,\text{lim}}$ and R are function of u_0 and C_0. Once $J_{v,\text{lim}}$ is known, the gel layer concentration C_g will be determined from Eq. (3).

For the purpose of illustration, consider the experimental data of Yeh and Cheng's work (13, 14) as follows: In their experimental work, an Amicon model H1P30-20 hollow-fiber cartridge (Amicon Corp., Danvers, MA) was used. The fiber (r_m = 0.025 cm, effective length L = 15.3 cm) was made of polysulfone and the total effective membrane area was 600 cm^2. The tested solute was dextran T500 (Pharmacia, M_n = 170,300 and M_w = 503,000). The solvent was deionized water. The concentrations of feed solutions were 0.1, 0.2, 0.5, 1.0, and 2.0 wt% dextran T500, the feed flow velocities were 0.051, 0.102, 0.204, and 0.306 m/s, and the feed inlet transmembrane pressures were 30, 50, 70, 100, and 140 kP$_a$. In all experiments the feed solution temperature was controlled at 25°C by a thermostat. The experimental data of solution permeate flux J_v obtained under various operating conditions are given in Table 1.

Figure 1 illustrates the method for determination of $J_{v,\text{lim}}$ and R for C_0 = 0.1 wt% and all values determined are listed in Table 2. Since R is a function of u_0 and C_0, Yeh and Cheng obtained the correlation equation for R from the experimental data as

$$R = 2.42 \times 10^9 + 7.49 \times 10^8 \, u_0^{-0.15} e^{0.87C_0} \ \text{P}_a\cdot\text{m}^2\cdot\text{s}\cdot\text{m}^{-3} \qquad (13)$$

Determination of C_g

According to conventional treatment of the gel polarization model, limiting permeate flux $J_{v,\text{lim}}$ vs ln C_b plots are straight lines as explained by Eq. (3), and these lines merge at one point on a concentration axis when J_v is zero, which gives the value of C_g. Many investigators pointed out that the values of C_g thus obtained are not the real concentrations in the gel layers because these values differ among membranes; some of the values are not realistic and can be larger than 100 wt% or less than zero (11, 15). Nevertheless, here we will merely consider the value of C_g as a parameter in the modified gel polarization model, and its value will be determined by an alternative way as follows.

Since the permeate flux J_v is low compared with the flow velocity u, we assume that the bulk concentration and velocity are approximately

TABLE 1
Permeate Flux for Dextran T500 Solution

	u = 0.051 m·s^{-1}			u = 0.102 m·s^{-1}			u = 0.204 m·s^{-1}			u = 0.306 m·s^{-1}		
C_0 (wt%)	ΔP kPa	$(J_v)_{exp}$ m^3·m^{-2}·s^{-1}	$(J_v)_{theo}$ × 10^{-6}	ΔP kPa	$(J_v)_{exp}$ m^3·m^{-2}·s^{-1}	$(J_v)_{theo}$ × 10^{-6}	ΔP kPa	$(J_v)_{exp}$ m^3·m^{-2}·s^{-1}	$(J_v)_{theo}$ × 10^{-6}	ΔP kPa	$(J_v)_{exp}$ m^3·m^{-2}·s^{-1}	$(J_v)_{theo}$ × 10^{-6}
0.1	25.1	3.40	3.18	24.1	3.82	3.56	22.5	4.02	3.86	20.4	3.98	3.87
	45.1	4.25	4.01	44.3	4.88	4.68	42.6	5.53	5.35	40.6	5.93	5.69
	65.1	4.78	4.46	64.3	5.61	5.30	62.7	6.44	6.22	60.5	6.95	6.75
	95.1	5.37	4.85	94.2	6.24	5.85	92.5	7.27	6.99	90.6	8.17	7.72
	135.0	5.83	5.13	133.8	6.76	6.26	132.3	7.99	7.59	130.3	9.08	8.47
0.2	25.2	2.70	2.81	24.0	3.08	3.17	22.5	3.40	3.49	19.8	3.35	3.46
	45.2	3.21	3.46	44.2	3.84	4.08	42.4	4.44	4.71	40.0	4.86	5.00
	65.2	3.54	3.80	64.2	4.30	4.56	62.2	4.96	5.39	60.1	5.62	5.86
	95.2	3.82	4.09	94.2	4.67	4.97	92.4	5.52	5.99	90.3	6.36	6.61
	135.1	4.20	4.30	134.0	5.09	5.27	132.1	6.07	6.43	130.3	7.02	7.18
0.5	24.5	2.02	2.18	23.5	2.29	2.58	21.3	2.55	2.76	18.5	2.64	2.76
	44.6	2.34	2.63	43.3	2.73	3.24	41.3	3.28	3.65	38.8	3.64	3.92
	64.7	2.50	2.85	63.4	2.99	3.59	61.5	3.62	4.11	58.5	4.14	4.50
	94.5	2.67	3.02	93.6	3.21	3.87	91.2	3.98	4.49	88.6	4.57	4.99
	133.9	2.86	3.15	134.0	3.46	4.08	131.7	4.28	4.77	128.7	5.00	5.35
1.0	24.3	1.54	1.60	22.8	1.73	1.84	20.0	1.92	2.03	16.5	1.85	1.99
	44.5	1.79	1.90	42.9	2.07	2.27	40.0	2.50	2.66	36.5	2.64	2.85
	64.2	1.93	2.03	62.9	2.29	2.47	60.0	2.78	2.97	56.4	3.03	3.26
	94.2	2.06	2.41	93.0	2.46	2.64	90.1	3.05	3.22	86.4	3.36	3.59
	133.7	2.18	2.22	133.0	2.62	2.76	129.9	3.24	3.39	126.4	3.62	3.82
2.0	23.6	1.09	0.86	21.1	1.21	0.98	16.5	1.26	1.03	21.6	1.60	1.28
	43.5	1.30	1.02	41.0	1.52	1.03	36.3	1.81	1.41	31.6	1.94	1.49
	63.5	1.43	1.10	61.1	1.69	1.31	56.3	2.06	1.58	51.3	2.34	1.71
	93.5	1.56	1.16	91.1	1.84	1.39	86.2	2.29	1.71	81.3	2.68	1.91
	132.7	1.66	1.20	131.1	1.96	1.45	126.0	2.49	1.80	121.4	2.92	2.03

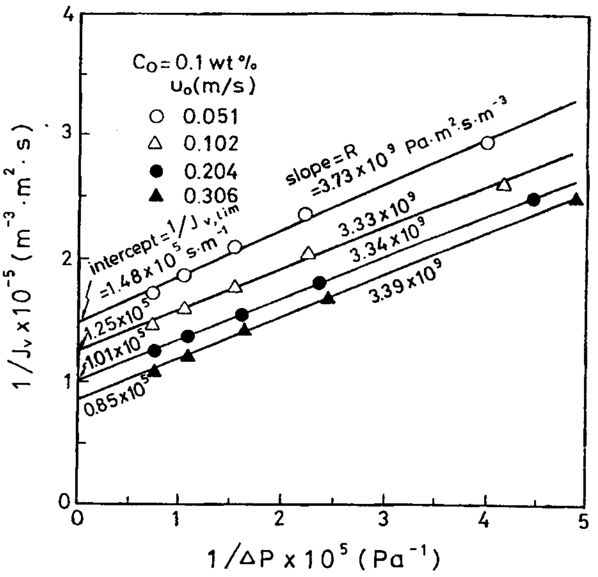

FIG. 1 Relation between $1/J_v$ and $1/\Delta P$.

the same as those of inlet values, i.e., $C_b \approx C_0$ and $u_b \approx u_0$. Further, the diffusivity coefficient in Eq. (2) is hard to estimate precisely because the concentration within the boundary layer is still uncertain. For convenience, here we evaluate the mass-transfer coefficient with the inlet value of the diffusion coefficient, D_0, and Eq. (3) is corrected by a modified factor F. Equations (2) and (3) become

$$k_0 = 1.62\left(\frac{u_0 D_0^2}{2r_m L}\right)^{1/3} \tag{14}$$

$$J_{v,\text{lim}} = k_0 F \ln\frac{C_g}{C_0} \tag{15}$$

or

$$J_{v,\text{lim}}/k_0 = F\ln C_g - F\ln C_0 \tag{16}$$

According to Eq. (16), if a straight line of $J_{v,\text{lim}}/k_0$ vs $\ln C_0$ can be constructed from the experimental data by the method of least squares, C_g and F can be determined because $\ln C_g$ is the intersection at the concentra-

TABLE 2
The Fitting Parameter of Experimental Data

C_0 (wt%)	u_0 ($m \cdot s^{-1}$)	$R \times 10^{-9}$ $Pa \cdot m^2 \cdot s \cdot m^{-3}$	$(1/J_{v,\lim}) \times 10^{-5}$ $s \cdot m^{-3}$	$J_{v,\lim}/k$
0.1	0.051	3.73	1.48	8.95
	0.102	3.33	1.25	8.41
	0.204	3.34	1.01	8.26
	0.306	3.39	0.85	8.57
0.2	0.051	3.95	2.17	6.01
	0.102	3.66	1.74	5.95
	0.204	3.42	1.43	5.75
	0.306	3.61	1.16	6.19
0.5	0.051	4.16	3.28	3.81
	0.102	4.06	2.66	3.53
	0.204	3.93	2.08	3.78
	0.306	3.81	1.74	3.95
1.0	0.051	5.51	4.24	2.76
	0.102	5.25	3.50	2.65
	0.204	4.92	2.74	2.69
	0.306	4.94	2.40	2.68
2.0	0.051	8.93	5.46	1.86
	0.102	7.75	4.58	1.80
	0.204	7.31	3.49	1.88
	0.306	7.38	2.82	2.03

tion axis, which gives the value of C_g, while $-F$ is the slope of this straight line.

The diffusion coefficient for a dextran T500 solution of concentration C_0 at 25°C can be estimated by the following correlation (16, 17):

$$D_0 \times 10^{11} = 1.204 + 0.2875C_0 - 5.042 \times 10^{-3}C_0^2 + 2.838 \times 10^{-5}C_0^3,\ m^2 \cdot s^{-1} \tag{17}$$

The experimental values of $J_{v,\lim}/k_0$ were calculated from Table 2 and Eqs. (14) and (17) with the given values $r_m = 2.5 \times 10^{-4}$ m and $L = 0.153$ m. The results are also presented in Table 2. The values of C_g and F for ultrafiltration of a dextran T500 solution in an Amicon model H1P30-20 hollow-fiber cartridge made of polysulfone were determined as shown in Fig. 2. The results are $C_g = 3.658$ wt% and $F = 2.194$.

Comparison of Theoretical Prediction with Experimental Data

The theoretical values of permeate fluxes for various feed concentrations and velocities were calculated based on the modified gel-polarization model shown by Eq. (4). The combined membrane resistance R was calculated from Eq. (13), and the limited permeate flux was evaluated from

$$J_{\mathrm{v,lim}} = 3.554\left(\frac{u_0 D_0}{2r_{\mathrm{m}}L}\right)^{1/3}\ln\left(\frac{3.658}{C_0}\right) \tag{18}$$

Equation (18) was obtained from Eqs. (14) and (15) with C_g and F replaced by 3.658 and 2.194, respectively. The theoretical results are presented in Table 1 for comparison with the experimental data. The theoretical predictions agree well in tendency with the experimental results.

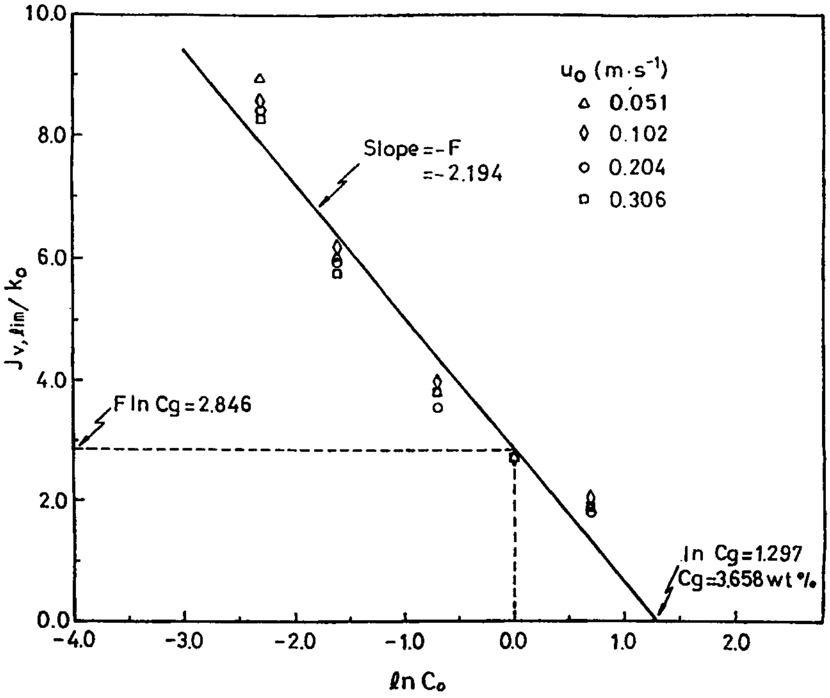

FIG. 2 Determination of C_g and F.

CONCLUSIONS

The effects of transmembrane pressure, flow velocity, and feed concentration on the permeate flux for ultrafiltration of aqueous solutions in hollow-fiber membrane modules have been investigated based on the modified gel-polarization model. It is found in this study that Eq. (4), as well as the modified gel-polarization model, successfully correlates the experimental results obtained for the ultrafiltration of a dextran T500 solution in an Amicon model H1P30-20 hollow-fiber cartridge made of polysulfone under certain experimental conditions. The equation for the limiting flux was also modified from Eq. (3), and a modified factor F was introduced as shown in Eq. (15). The gel-layer concentration C_g and the modified factor F were determined by an unconventional, but rather convenient, method as shown in Fig. 2.

Since the conventional gel-polarization model only applies to membrane ultrafiltration under high-pressure operation, and the permeate flux $J_{v,\mathrm{lim}}$ defined in this model is independent of transmembrane pressure, practical application is limited and not quite suitable for analysis of membrane ultrafiltration. The modified gel-polarization model introduced in the present work extends the application to even lower transmembrane pressures. Furthermore, since the modified gel-polarization model easily describes the relationships of permeated flux with operating parameters, we believe that this model will also be suitable for most membrane ultrafiltration systems, including systems with different kinds of feed solutions, different materials of hollow fiber, and various design and operating conditions.

SYMBOLS

C_0	solute concentration at the inlet (wt%)
C_b	bulk solute concentration (wt%)
C_g	solute concentration in the gel layer (wt%)
C_m	solute concentration on membrane surface (wt%)
D	diffusion coefficient ($m^2 \cdot s^{-1}$)
D_0	diffusion coefficient at the inlet ($m^2 \cdot s^{-1}$)
F	modified factor defined by Eq. (15)
J_v	volume permeate flux for solution ultrafiltration ($m^3 \cdot m^{-2} \cdot s^{-1}$)
$J_{v,\mathrm{lim}}$	limiting volume permeate flux ($m^3 \cdot m^{-2} \cdot s^{-1}$)
k	mass transfer coefficient ($m \cdot s^{-1}$)
k_0	mass transfer coefficient at the inlet ($m \cdot s^{-1}$)
L	length of hollow fiber (m)
P_L, P_0	outlet, inlet pressure of the tubeside (Pa)
P_p	permeate pressure of the shellside (Pa)
ΔP	transmembrane pressure defined by Eq. (9) (Pa)

R	combined membrane resistance, $R_f + R_m$ ($Pa \cdot m^2 \cdot s \cdot m^{-3}$)
Re	Reynolds number
R_f	resistance due to solute adsorption and fouling ($Pa \cdot m^2 \cdot s \cdot m^{-3}$)
R_m	intrinsic resistance of membrane ($Pa \cdot m^2 \cdot s \cdot m^{-3}$)
r_m	radius of hollow fiber (m)
Sc	Schmidt number
u	flow velocity ($m \cdot s^{-1}$)
u_0	feed flow velocity ($m \cdot s^{-1}$)

REFERENCES

1. M. C. Porter and A. S. Michaels, "Membrane Ultrafiltration, Part 1," *Chem tech*, p. 56 (January 1971).
2. M. C. Porter and A. S. Michaels, "Membrane Ultrafiltration, Part 2," *Ibid.*, p. 248 (April 1971).
3. M. C. Porter and A. S. Michaels, "Membrane Ultrafiltration, Part 3," *Ibid.*, p. 44 (July 1971).
4. M. C. Porter and A. S. Michaels, "Membrane Ultrafiltration, Part 4," *Ibid.*, p. 633 (October 1971).
5. M. C. Porter and A. S. Michaels, "Membrane Ultrafiltration, Part 5," *Ibid.*, p. 56 (January 1972).
6. A. S. Michaels, "New Separation Technique for the CPI," *Chem. Eng. Prog.*, *64*(12), 31 (1968).
7. M. C. Porter, "Concentration-Polarization with Membrane Ultrafiltration," *Ind. Eng. Chem., Prod. Res. Dev.*, *11*, 234 (1972).
8. P. J. Flory, *Principles of Polymer Chemistry*, Cornell University Press, Ithaca, New York, 1953, p. 279.
9. C. Tanford, *Physical Chemistry of Macromolecules*, Wiley, New York, 1961.
10. L. Graetz, "Uber die Waermeleitungsfaehigkeit von Fluessigkeiten, Part I," *Ann. Phys. Chem.*, *18*, 79 (1883).
11. H. Nabetani, M. Nakajima, A. Watanabe, S. Nakao, and S. Kimura, "Effects of Osmotic Pressure and Adsorption on Ultrafiltration of Ovalbumin," *AIChE J.*, *36*, 907 (1990).
12. B. H. Chiang and M. Cheryan, "Ultrafiltration of Skimmilk in Hollow Fibers," *J. Food Sci.*, *51*(2), 340 (1986).
13. H. M. Yeh and T. W. Cheng, "Resistance-in-Series for Membrane Ultrafiltration in Hollow Fibers of Tube-and-Shell Arrangement," *Sep. Sci. Technol.*, *28*(6), 1341 (1993).
14. T. W. Cheng, "A Study of the Hollow-Fiber Membrane Ultrafiltration," Ph.D. Dissertation, National Taiwan University, Taipei, Taiwan, Republic of China, 1992.
15. S. Nakao, T. Nomura, and S. Kimura, "Characteristics of Macromolecular Gel Layer Formed on Ultrafiltration Tubular Membrane," *AIChE J.*, *25*(4), 615 (1979).
16. J. G. Wijmans, S. Nakao, J. W. A. Van Den Berg, F. R. Troelstra, and C. A. Smolders, "Hydrodynamic Resistance of Concentration Polarization Boundary Layers in Ultrafiltration," *J. Membr. Sci.*, *22*, 117 (1985).
17. H. M. Yeh and T. W. Cheng, "Osmotic-Pressure Model with Permeability Analysis for Membrane Modules Ultrafiltration in Hollow-Fiber," *Sep. Technol.*, *3*, 91 (1993).

Received by editor March 8, 1994
Revision received May 29, 1995